ACS APPLIED MATERIALS & INTERFACES

Research Article

www.acsami.org

Control Performance of Paper-Based Blood Analysis Devices through Paper Structure Design

Lizi Li,[†] Xiaolei Huang,[‡] Wen Liu,[‡] and Wei Shen*,[†]

[†]Department of Chemical Engineering, Monash University, Clayton Campus, Clayton, VIC 3800, Australia

[‡]China National Pulp and Paper Research Institute, Beijing 100102, China

Supporting Information

ABSTRACT: In this work, we investigated the influence of paper structure on the performance of paper-based analytical devices that are used for blood analysis. The question that we aimed to answer is how the fiber type (i.e., softwood and hardwood fibers) influences the fiber network structure of the paper, which affects the transport of red blood cells (RBCs) in paper. In the experimental design, we isolated the influence of fiber types on the paper structure from all other possible influencing factors by removing the fines from the pulps and not using any additives. Mercury porosimetry was employed to characterize the pore structures of the paper sheets. The results show that papers with a low basis weight that are made with short hardwood fibers have a higher porosity (i.e., void fraction) and simpler pore structures compared with papers made with long softwood fibers. RBC transport in paper carried by saline solution was investigated in two modes: lateral chromatographic elution and vertical flow-through. The results showed that the complexity of the paper's internal pore structure has a dominant influence on the transport of RBCs in paper. Hardwood fiber sheets with a low basis weight have a simple internal pore structure and allow for the easy transport of RBCs. Blood-typing sensors built with low basis weight hardwood fibers deliver high-clarity assays. Softwood fiber papers are found to have a more complex pore structure, which makes RBC transport more difficult, leading to blood-typing results of low clarity. This study provides the principle of paper sheet design for paper-based blood analysis sensors.

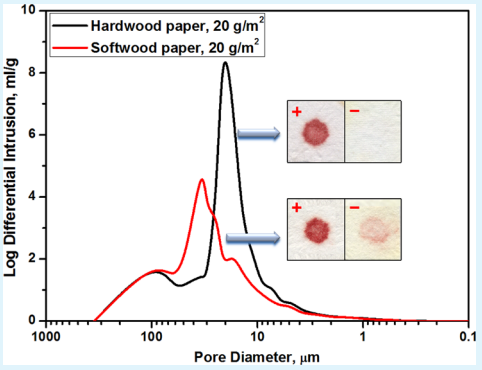

KEYWORDS: *paper-based diagnostic sensors, paper structure, hardwood fiber, softwood fiber, blood typing, mercury porosimetry*

1. INTRODUCTION

Paper-based microfluidic devices and paper-based sensors have attracted a lot of attention because of their potential applications in point-of-care, immunoassays, food-quality testing, environmental monitoring, and disease screening in resource-limited areas.[1−10] Paper made of cellulose fibers demonstrates significant advantages over other substrates, such as silicon and glass, when used in the manufacturing of low-cost, disposable, and flexible diagnostic devices.[1,2,11−13] Paper-based sensors use the hydrophilic nature of the cellulose fiber network to transport homogeneous aqueous liquids by capillary wicking. To control the direction of liquid wicking on paper, previous publications reported a variety of methods to pattern the paper.[1,14−17] By physically and chemically functionalizing paper and patterned paper devices, many routine chemical and biological assays can be performed using paper-based devices without the need for sophisticated analytical equipment.[1,9−11] More recently, paper-based microfluidic diagnostics has evolved from analyzing samples of very simple matrices to analyzing samples of more complex matrices, such as animal and human blood samples.[18−20] Paper-based device design has increasingly involved the use of a colloid suspension, such as metal nanoparticles and encapsulated functional nanoparticles, as the reaction media or indicator system.[21,22] Although several methods of using paper to separate and analyze heterogeneous samples have been demonstrated, the physicochemical properties of paper that are best-suited for analyzing a heterogeneous sample are not yet fully understood.[1] Paper is a material with a three-dimensional porous structure that is formed by multiple layers of cellulosic fibers.[23,24] It has been used for a long time as a filtration medium for separating solid and colloidal particles from heterogeneous fluids. To better utilize the filtration property of the paper to design high-performance paper sensors for complex sample analysis, a detailed understanding of the fiber network structure and particle transport behavior in paper is necessary.

Our group has developed a series of paper-based fluidic devices for blood typing; these devices work based on filtration and chromatographic separation principles.[8,18,19,25] Whole human blood is composed of a continuous plasma phase with red blood cells (RBCs) in a suspension state. The blood group is classified on the basis of the inherited differences (polymorphisms) in the antigens on the surface of the RBCs.[26−28]

Received: September 26, 2014
Accepted: November 18, 2014
Published: November 18, 2014

Whereas the biochemical basis of a paper-based blood-typing assay is the hemagglutination of RBCs by their corresponding grouping antibodies, the mechanism of interpreting the assay result relies on the transport behaviors of agglutinated RBC lumps and nonagglutinated free RBCs within the porous fiber network of the paper. Paper-based blood-typing devices are fabricated by simply imbibing blood group antibody solutions into the fiber network of a paper. In a blood-typing assay, a blood sample is allowed to imbibe into the paper that has been treated with the antibodies. This design concept allows the hemagglutination to occur inside the fiber network of the paper. For a positive assay, hemagglutination makes RBCs agglutinate via the intercellular cross-linking by their corresponding antibody molecules. The agglutinated RBC lumps are then immobilized primarily by mechanical entrapment in the porous structure of paper. In contrast, no hemagglutination occurs in a negative assay; nonagglutinated RBCs remain stably dispersed in the plasma phase and can move through porous fiber network of paper, with plasma occurring as a single suspension phase.[18,25,29] To display the blood-typing result, the assay is subjected to either a buffer elution in a chromatographic tank or a buffer rinsing step to allow a small volume of buffer to penetrate the paper. Buffer elution or buffer rinsing is intended to flush out free RBCs from the fiber network. Because only nonagglutinated RBCs are free in the fiber network and agglutinated RBC lumps are not, a chromatographic elution or buffer rinsing can provide visual evidence of the occurrence of hemagglutination: a negative assay should show no blood color on the paper, whereas a positive result should show a strong blood color.[18,19]

A successful blood-typing assay on paper must differentiate a positive assay from a negative one with high clarity. In our investigation, we observed that blood-typing assay clarity is dependent on the type of paper selected. Visually, low clarity means that a negative assay may carry a faint to moderate blood color, whereas a positive assay occasionally gives a low density of the blood color; these observations may lead to an ambiguous assay result. To improve the clarity of the paper-based blood-typing assays, paper structures must be characterized and their influence on the movements of RBCs must be understood. This understanding will provide key information not only for selecting the right papers to fabricate blood-typing devices but also for fabricating paper-based devices for other blood analyses.

A paper sheet is often considered as an infinite network in its lateral dimensions but finite in the vertical (or z) direction.[24] Because paper-based blood-typing devices typically adopt two different designs, i.e., the lateral chromatographic flow design[8,18] and the vertical flow-through design,[19,25] the paper structure may influence the sample flow and the RBC separation of these flow modes differently, due to the anisotropic structural characteristics of paper.

In an actual papermaking process, a variety of chemical additives are used to improve the paper sheet properties, which include the wet and dry strength and printability additives. These additives include cationic starch, sodium carboxymethyl cellulose (CMC), and cationic polymers, such as polyacrylamide (PAM) and poly(diallyl dimethylammonium chloride) (PDADMAC).[13,30,31] Wood pulps also contain a fraction of fine fibrous and granular particles known as fines. However, for the papers that are used for blood typing, the charges carried by additives may affect the transport behavior of RBCs in fiber networks because RBCs are negatively charged in the plasma environment.[28] Fines may also interact with fibers and RBCs. Because of the above factors, no commercial paper possesses the optimized properties for blood-typing assays.

In this work, we investigate the effect of paper structure on the performance of paper-based blood-typing devices. Papers with different basis weights were made using different fibers. To clearly identify the influence of the paper's physical structures on its blood-typing performance, no chemical additives were used and the fine particles in the pulp were removed in this study. The paper sheet properties were characterized with apparent thickness and apparent bulk measurements and with mercury intrusion porosimetry. Blood-typing assays by lateral chromatographic elution and vertical flow-through modes were investigated to study the red blood cell transport behavior in the papers' internal porous structure and the paper-based sensor performance.

2. EXPERIMENTAL SECTION

2.1. Materials. Eucalyptus hardwood bleached kraft pulp and northern softwood bleached kraft pulp were obtained from the National Institute of Standards and Technology (Gaithersburg, MD). The properties of these pulps were retrieved from the reports of NIST standard reference materials 8495 and 8496. Standard blotting paper with a basis weight of 280 g/m^2 was obtained from Fibrosystem AB and used as the absorbent paper for making handsheets. Blood samples were collected from adult volunteers with known blood groups through Red Cross Australia. All blood samples were stabilized with anticoagulant additives, stored in Vacutainer test tubes containing heparin, citrate, and EDTA at 4 °C and used within 7 days of collection. ALBAclone anti-A (Z001), anti-B (Z011), and anti-D (Z039) monoclonal grouping reagents were sourced commercially from Alba Bioscience Ltd. Anti-A and anti-B are a transparent cyan and a transparent yellow solution, respectively, whereas anti-D is a colorless solution. Monoclonal grouping reagents were also kept at 4 °C. Analytical grade NaCl from Sigma-Aldrich was used to prepare the physiological saline solution.

2.2. Methods. Hardwood and softwood fibers were obtained by disintegrating hardwood and softwood pulps using a Messmer standard pulp disintegrator for 7500 revolutions. The fibers were then thoroughly washed with a 150-mesh to remove the fines. Handsheets with basis weights of 20, 35, and 50 g/m^2 were made with hardwood and softwood fibers. Handsheets (20 g/m^2) with different contents of hardwood and softwood fibers were also made. TAPPI (Technical Association of the Pulp and Paper Industry) standard method T205 was followed for making the handsheets. All handsheets were conditioned at 23 °C and 50% relative humidity for 24 h before measuring their physical properties. The sheet basis weight, apparent thickness, and apparent bulk were measured following the TAPPI standard method T220. The terms "thickness" and "bulk" used below indicate the "apparent thickness" and "apparent bulk". The mercury intrusion measurements were performed using an AutoPore IV 9500 instrument (Micrometritics).

For the lateral chromatographic elution test, paper handsheets were cut into 100 × 30 mm^2 strips. Ten microliters of antibody solution was spotted 2 cm from the shorter side of the paper strip and allowed to be absorbed completely over 30 s. An aliquot of 1 μL of whole blood sample was dropped onto the center of the antibody spot and allowed to react with the antibody reagent for 30 s. Then, the paper strip was suspended in a physical saline solution in a chromatographic tank to allow elution for 90 s; the distance between the blood spot and the level elution buffer was kept at 10 mm. The paper strip was then removed from the chromatographic tank and suspended in a fume cupboard to be dried in air at room temperature for 10 min. The dried paper strip was then scanned using a scanner (Epson Perfection 2450) for image analysis.

For the vertical flow-through saline-rinsing blood-typing test, handsheets were cut into 10 × 10 mm^2 paper squares. The testing paper was prepared by adding 10 μL of antibody solution to the paper

surface and allowing it to dry in air for 3 min. One microliter of whole blood sample was introduced onto the paper and allowed to react with the antibody reagent for 30 s. The testing paper was then transferred onto a sheet of blotting paper to perform the saline rinsing. Rinsing was performed by introducing a total of 30 μL of saline solution onto the center of the blood spot for two applications; the absorbing power of the blotting paper assisted the rinsing buffer to penetrate through the testing paper. The rinsed blood-testing paper was allowed to dry in the fume cupboard for 10 min. A scan of the dried testing paper was then obtained.

The optical density values of blood spots of the positive and negative assays were assessed and reported as the mean ± SD (standard deviation). Unpaired two-tailed *t* tests were used to compare the mean optical density values for the analysis of different blood samples with different testing modes. One-way analysis of variance (ANOVA) was applied to compare the mean red color optical density in more than two groups. The statistical analysis was performed using the GraphPad Prism (version 6) software with $P < 0.05$ considered significant.

3. RESULTS AND DISCUSSION

3.1. Isolation of the Paper Physical Structure from the Influence of Chemical Additives and Fines. To gain a precise understanding of the influence that the paper sheet physical structure has on its bloodtyping performance, we formed handsheets using well-characterized softwood and hardwood pulps, but without using any additives. Fines were also removed because their contribution to RBC transport should be investigated separately.

Handsheets with basis weights of 20, 35, and 50 g/m^2 were made with hardwood and softwood fibers, respectively. Figure 1a shows that the apparent thickness of the handsheets increased substantially with the increase in sheet basis weight. For hardwood handsheets, when the basis weight was increased from 20 to 50 g/m^2, the thickness increased from 84.9 to 171.9 μm, representing an increase of 102.5%. For handsheets made from softwood fibers, a similar trend can be observed. This trend is intuitively appreciable because the number of fiber layers increases with the basis weights of handsheets. Figure 1a also shows that all of the hardwood handsheets have greater apparent thickness compared with the softwood handsheets of the same basis weight. Figure 1b shows that for each basis weight, hardwood sheets have a higher bulk value than do the softwood sheets. The bulk of a paper is defined as the reciprocal of the sheet density and has a unit of cubic centimeters/gram.[32] Additionally, the bulk of the hardwood and softwood handsheets decreased from 4.13 to 3.36 cm^3/g and from 3.88 to 3.07 cm^3/g, respectively, as the sheet basis weights increased to 50 g/m^2. The data in Figure 1b indicate that the volume of voids in a hardwood sheet was higher than that in a softwood sheet of the same basis weight. It also indicates that the fiber network became denser as the sheet basis weight increased.

Figure 2 shows the thickness and bulk of handsheets made of different blends of hardwood and softwood fibers, all with a basis weight of 20 g/m^2. The thickness of the handsheets increases with the content of hardwood fibers to 50% at first and then levels off. It, however, is only suggested because the error bars of some data sets are large. Detailed handsheet data can be found in Table S3 in the Supporting Information (SI). By varying the sheet thickness and bulk through controlling the content of different fibers, the structure of the paper network can be varied in a controlled manner. This provides the possibility to investigate the influence of the paper's physical structure on the transportation and immobilization of RBCs, without any interference from chemical additives.

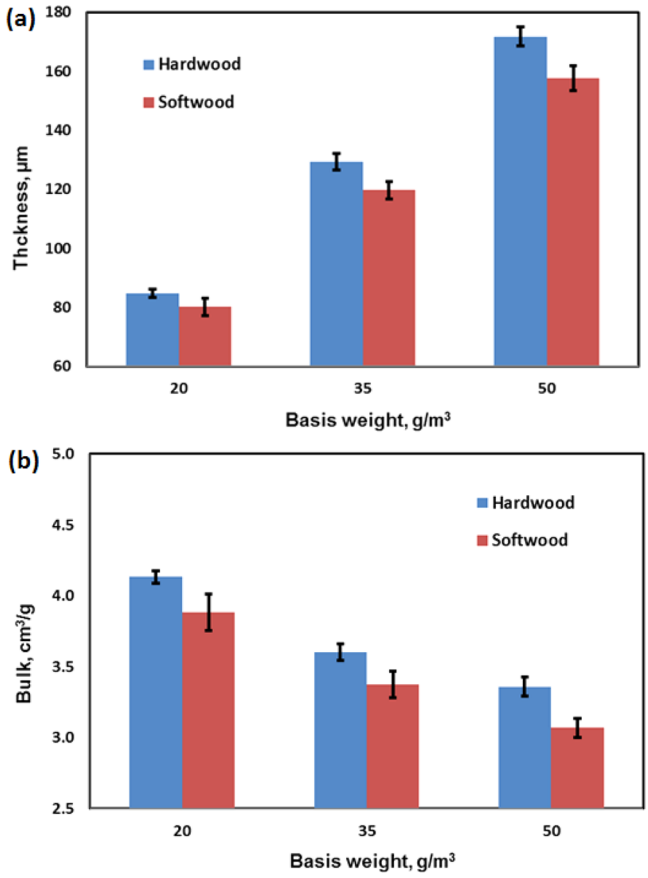

Figure 1. Apparent thickness (a) and apparent bulk (b) of hardwood and softwood handsheets of different basis weights.

3.2. Characterization of Pore Size Distribution of Paper. Mercury porosimetry was used to characterize the pore size distribution of handsheet samples. Figure 3a shows the pore size distributions of hardwood handsheets of different basis weights. The data show similar bimodal patterns. Such a pattern has been reported previously.[33] Silvy et al. attributed the low-intensity peak of larger pore diameters to the pores located on the surface of the paper and the high-intensity peak of smaller pore diameters (between 10 and 30 μm) to pores inside the sheets.[33] Our results show that both peaks for hardwood 20 g/m^2 paper are higher than those of papers with higher basis weights; this finding indicates that papers with lower basis weight have a more porous surface and internal structures. This finding is in agreement with the sheet bulk results shown in Figure 1b.

The sizes of the surface pores of hardwood paper are centered at approximately 100 μm and range from 45 to 200 μm. Because RBCs have the shape of biconcave disks, with a diameter of 6−8 μm and a thickness of 2 μm,[29] they can easily pass through the surface pores of hardwood paper. Furthermore, the integral of the log differential intrusion plot over a certain pore size range gives the cumulative mercury intrusion volume; it reflects the pore volume corresponding to the pore size range of the material being tested.[34] Because the 20 g/m^2 hardwood handsheet has the highest volume of surface pores, it could therefore be hypothesized to have a greater capability to allow for the lateral transportation of free RBCs via chromatographic elution.

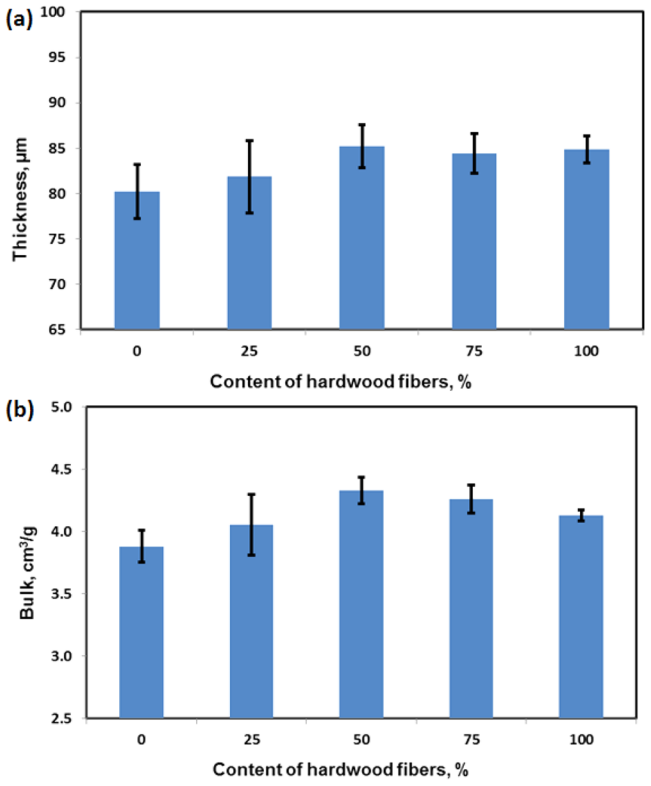

Figure 2. Apparent thickness (a) and apparent bulk (b) of handsheets with different content of hardwood and softwood fibers (basis weight of all sheets was 20 g/m^2).

Figure 3a also shows that the internal pores of hardwood handsheets with basis weights of 20, 35, and 50 g/m^2 are centered at 20, 18, and 10 μm, respectively. Among these handsheets, the 20 g/m^2 one has an internal volume of 8.4 mL/g, while the internal volumes of the 35 and 50 g/m^2 sheets are much lower, being 4.7 and 4.2 mL/g, respectively. In addition, the high-intensity peak of the 20 g/m^2 hardwood handsheet is narrower than those of higher basis weights. These findings suggest that low basis weight handsheets have more uniform internal pore size distribution, which is a desirable sheet property for separation. It is noted, however, that the internal pore size distribution of the 50 g/m^2 hardwood sheet has a shoulder, suggesting that the internal structure is formed by pores of two sizes. We hypothesized that the internal pore structure of the 50 g/m^2 hardwood sheet was less uniform and more complex. One explanation of this observation is that sheets of high basis weight contain more fibers, which contribute to more fiber−fiber bonding; this leads to a more complex internal pore structure of the sheet. We hypothesize that RBC transport in complex pore structures would be more difficult. This effect is discussed in more detail below.

Internal pores with diameters smaller than 8 μm would not provide easy transport pathways to free RBCs. Although it is known that red cells can pass through veins with smaller diameters than those of RBCs under pressure through cell deformation,[35,36] no report has shown that this would also occur for RBCs traveling in a porous network under no external pressure.

In summary, hardwood handsheets of lower basis weights could have the potential to transport free RBCs more efficiently via both chromatographic elution and flow-through modes

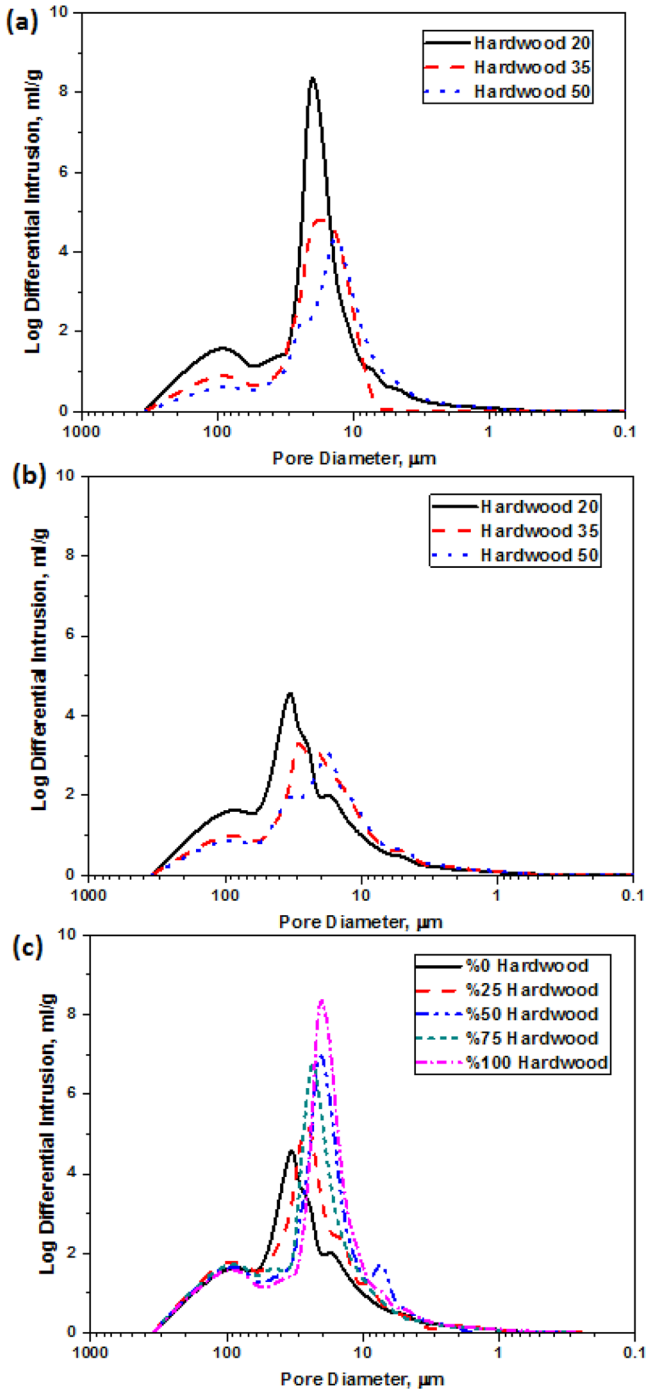

Figure 3. Pore size distributions of (a) hardwood paper with different basis weights, (b) softwood paper with different basis weights, and (c) paper with different content of hardwood and softwood fibers (basis weight of 20 g/m^2).

because of their large surface volume and internal pores that have uniform sizes.

The pore size distributions of softwood papers are illustrated in Figure 3b. The first (left) peak corresponds to surface pores; the second peak with more than one shoulder corresponds to the internal pores. The pore volume of softwood handsheets decreases as the basis weight increases; this trend is similar to that observed for hardwood sheets. This trend indicates that sheets of higher basis weights contain more fibers and therefore more fiber−fiber bondings, which leads to denser sheets (see

also Figure 1b). This finding is in agreement with the sheet bulk data in Figure 1b.

The first peak of surface pores of softwood paper is also centered at approximately 100 μm, similar to that of the hardwood paper. The most interesting information in Figure 3b, however, is that the mercury intrusion results show more than one peak in the region of internal pores, indicating that the internal pore structures of the softwood sheets are more complicated than those of hardwood sheets and that mercury intrusion into the softwood handsheets has met a hierarchical internal structure. This can be clearly observed from the four peaks (shoulders) of the intrusion curve for the internal pore region of the 20 g/m^2 softwood sheet. At the end of each step of the hierarchical structure, the rate of mercury intrusion slowed down, but the rate increased again when mercury intruded into the pores of the next hierarchical step. This could make the transport of RBC in softwood sheets more difficult. The mercury intrusion results are discussed with respect to the RBC elution results below.

The pore size distributions of papers made by blending hardwood and softwood fibers in different proportions were also analyzed using mercury porosimetry, and the results are presented in Figure 3c. The basis weight of all of the sheets made with mixed fibers was 20 g/m^2. The results show that mixing short and long fibers in different proportions does not change the size or volume of the surface pores. Thus, the surface pores are dominantly determined by the basis weight of the sheets and sheet-forming conditions, but not by the fibers. Figure 3c also shows three expected trends. First, as the percentage of long softwood fibers in the handsheets increases, the overall pore volume of the sheets decreases. This trend is supported by the conclusion of the previous section that long softwood fibers form denser sheets. Second, the pore size of handsheets increases with an increase in the percentage of softwood fibers. This trend can be explained as follows: the pore size of a network structure formed with larger fibers (both in length and in width) is larger than that formed with smaller fibers. Third, the internal sheet structure becomes increasingly complex as the percentage of long fibers is increased to above 50%. This trend is supported by the increased fiber network hierarchical structure with the increase of long fibers in the network.

With the above insights into the handsheet surface and internal structures, we have made hypotheses concerning RBC transport behavior in different sheets. Tests of these hypotheses are presented below.

3.3. Effect of the Physical Structure of Paper on Lateral Elution Blood-Typing Performance. In the lateral chromatographic elution blood-typing test, blood was spotted onto a handsheet treated with grouping antibody reagents; the spotted sheet was then chromatographically eluted by physical saline solution in a chromatographic tank for 90 s. A blood sample spotted on its corresponding antibody will agglutinate and become immobilized on the same spot in paper and resist saline elution; this signifies a positive test result. Conversely, a blood sample spotted onto noncorresponding antibodies will not agglutinate; RBCs remain free and can be eluted away by the saline buffer, leaving behind no, or a very faint, blood spot. Such an assay signifies a negative result. The critical criterion of a high-performance blood-typing device is the ability to distinguish a positive result from a negative result with high clarity. Both surface and internal pores of paper affect the fixation and transport of agglutinated and free RBCs.

From Figure 4a, the positive and negative results for the 20 g/m^2 hardwood paper had the highest clarity judged by naked eye, whereas the results for the 50 g/m^2 softwood sheet had the lowest clarity. Quantitative analysis of optical density of the blood spotting area is given in Figure 4b and Table S3 in the SI. The optical densities of all positive tests were high and not significantly affected by either sheet basis weight or fiber type. However, the optical density of all negative tests increased substantially with an increase in sheet basis weight. In addition, the scanned images of chromatographically eluted blood spots on handsheets containing different percentages of softwood fibers (Figure 5a) show that although the positive tests on all sheets have high optical density (Table S4, SI), the optical density of negative results increases with the increase in softwood fiber content; this reduces the clarity of the negative tests. Therefore, for sheets of the same basis weight, their chromatographic elution performance reduces as the content of the softwood fiber in the sheet increases.

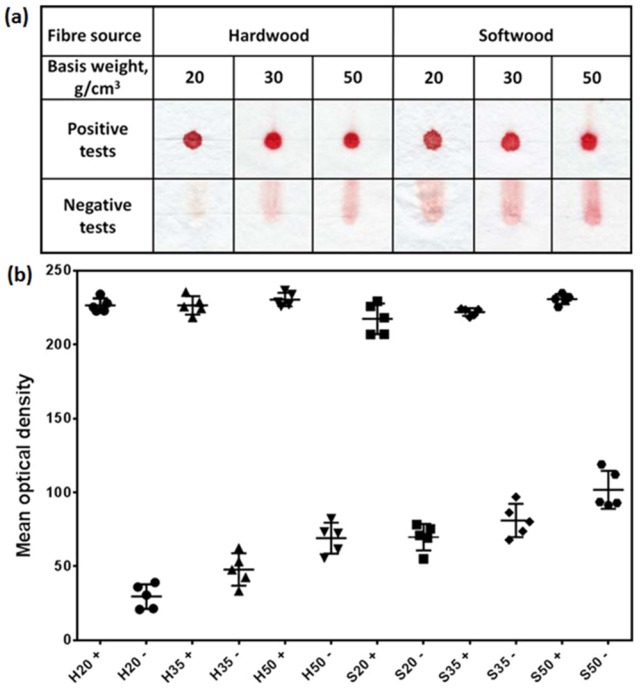

Figure 4. Lateral chromatographic elution blood-typing tests using papers of different basis weights: (a) scanned images of testing results and (b) mean optical densities of positive (+) and negative (−) tests. H, hardwood fibers; S, softwood fibers. The numbers after H and S are the basis weights of papers in g/m^2.

To interpret the above results, the following points are considered. First, the reason why positive tests are less affected by the physical structure of paper sheets is because the RBC reacted with the corresponding antibody and agglutinated into large aggregates. Our previous confocal microscopy study revealed that agglutinated RBC aggregates were immobilized inside the fiber network through entrapment in interfiber gaps and adhesion to the fiber surface.[29,40] Those immobilized RBC aggregates could not be moved by capillary-driven buffer elution. Therefore, the physical properties of paper sheets have a weak influence on the clarity of positive tests performed using the chromatographic elution method.

Second, the physical structure of the paper substrate plays a significant role in the elution of nonagglutinated RBCs in a

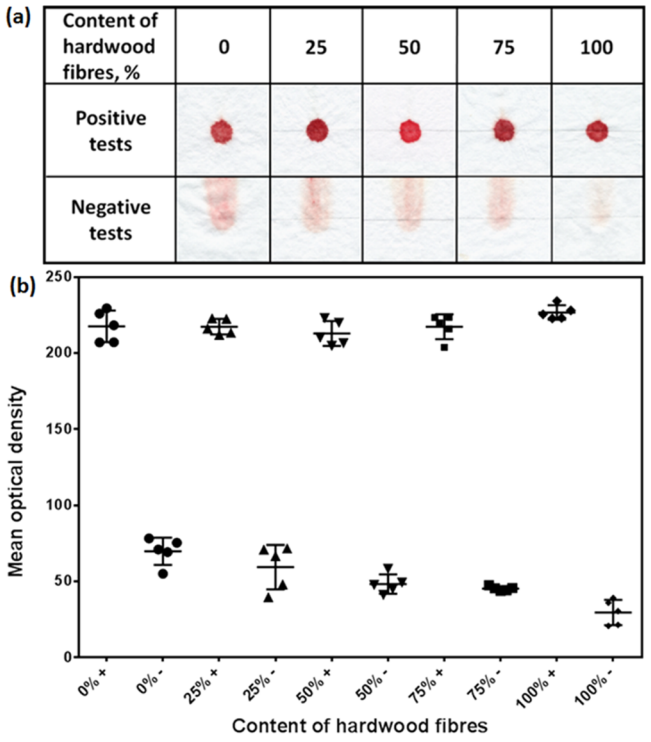

Figure 5. Lateral chromatographic elution blood-typing tests using paper with different content of hardwood fibers: (a) scanned images of testing results and (b) mean optical densities of positive (+) and negative (−) tests.

negative test using the chromatographic elution method. Mercury intrusion results of handsheets made with different fibers and mixed fibers showed that most internal pores of all sheets are sufficiently large for free RBCs to pass through. However, the internal pore structures became more complicated as the content of softwood fibers increased (Figures 3c and 5) and as the sheet basis weight increased (Figures 3a,b and 4). Because the movement of RBCs in the fiber network is driven by the capillary flow of the plasma phase, it will be slowed down when the network becomes more complex.

Roberts et al.[37] showed that the penetration of aqueous liquid in paper was by film flow. V-shaped microgrooves formed by the interfiber gaps constitute a major group of channels for liquid transport in paper. Their model shows that liquid wicking along a fiber gap is interrupted or stopped when the liquid wicking front hits the discontinuity of a V-groove channel. Roberts et al. showed that fiber−fiber crossing points could be points of discontinuity, which could cause the liquid wicking front to stop and then change to another channel to continue the wicking.[37] In our study of blood wicking in paper, RBCs are likely to be caught at the fiber−fiber crossing points where the buffer wicking front hits points of discontinuity. This will increase the chance for more and more RBCs to be left behind the buffer wicking front, reducing the clarity of a negative blood-typing assay by chromatographic elution.

Softwood fibers are approximately three times longer and are thicker than hardwood fibers.[38] In a paper sheet, a single softwood fiber may have more fiber−fiber crossing points than a single hardwood fiber because of the greater length of the former. He et al. and Batchelor et al. proposed a new analytical model that links the paper sheet cross-sectional properties of the fibers in the sheet to the number of fiber−fiber crossing points per unit length of fiber; their modeling work concluded that the number of fiber−fiber crossing points along a single softwood fiber in a sheet is greater than that along a hardwood fiber.[39] This greater number leads to a larger number of liquid flow discontinuities along a single softwood fiber than a single hardwood fiber. Because of the greater width of a softwood fiber compared with a hardwood fiber, the fiber−fiber contact area of two crossing softwood fibers is greater than those of two crossing hardwood fibers. Therefore, fiber−fiber crossings formed by softwood fibers present more substantial discontinuities to the liquid flow and RBC migration. In this study, the observed more complex internal pore structures of softwood fiber sheets agree with the above analysis. Therefore, buffer wicking in paper sheets with higher softwood fiber content will meet a greater number of discontinuities. This creates more obstacles to the elution of free RBCs, resulting in negative elution blood typing with low clarity. Increasing the sheet basis weight has a similar effect.

In summary, a paper's physical structure affects the clarity of positive tests of chromatographic elution blood typing relatively weakly, but it affects the clarity of negative tests significantly. Our investigation shows that paper sheets of low basis weight and high hardwood fiber content provide greater assay clarity for chromatographic elution blood typing. The results from this study provide a guide for the future investigation of paper chemical effects on elution blood typing.

3.4. Effect of Paper Physical Structure on Vertical Flow-Through Blood-Typing Performance. An advantage of the flow-through test over the lateral elution test in practical blood-typing application is its rapidness; test results can be read immediately after rinsing. The mechanism of buffer rinsing and buffer elution is different, and the influence of paper properties on the clarity of flow-through rinsing results is thus different.

For the buffer rinsing method, the buffer does not just enter the pores in a paper sheet by capillary wicking. Instead, when a drop of buffer is added to the blood spot on paper surface, it floods the blood spot. Because the agglutination of RBCs by their corresponding antibodies is a reversible process, some large lumps of agglutinated RBCs may dissociate into smaller ones or even to free RBCs when flooded by buffer and be flushed away by the rinsing buffer. Figure 6a shows that the color densities of positive assays obtained using the rinsing method are weaker than those obtained using the elution method for the same handsheets, whereas the clarity of negative assays was improved.

The antibody concentration in the paper sheet is likely to be the major factor affecting the color density of positive assays. Because buffer rinsing can cause the dissociation of agglutinated RBCs, a higher antibody concentration in the sheet will resist such dissociation by shifting the equilibrium toward the RBC agglutination. In the antibody treatment of the sheets, the same quantity of antibody solutions was added to sheets of different basis weights, which have different thickness (Figure 1a). Our experimental observation showed no significant difference in sizes of antibody-wetted areas on sheets of different basis weights. Considering that low basis weight sheets have low thickness, the antibody would be distributed in a smaller volume; the antibody concentration in low basis weight sheets is likely to be higher than that in high basis weight sheets. Because the RBC agglutination is controlled by the equilibrium involving the antibody concentration, it is expected that the RBC agglutination on the 20 g/m^2 sheets would be the strongest. The results of optical density for positive tests in

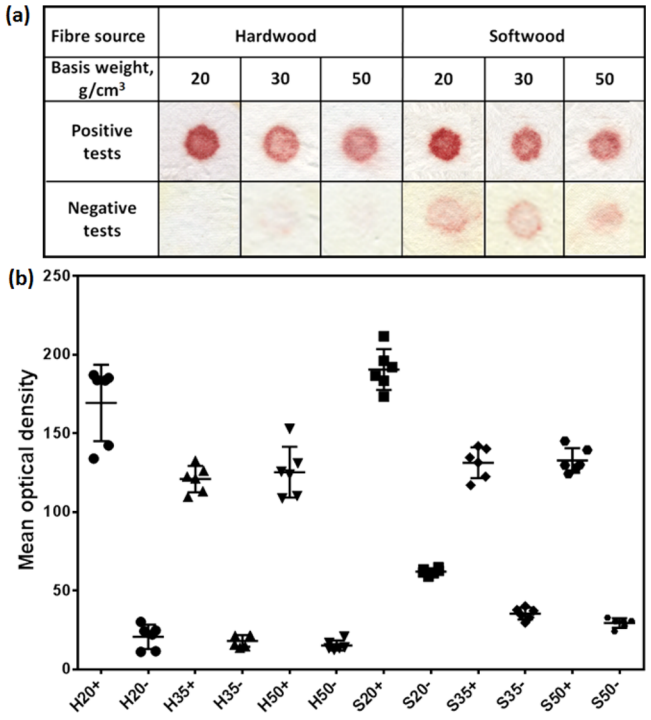

Figure 6. Vertical flow-through blood-typing tests using paper of different basis weights: (a) scanned images of testing results and (b) mean optical densities of positive (+) or negative (−) tests. H, hardwood fibers; S, softwood fibers. The numbers after H and S are basis weight of papers in g/m^2.

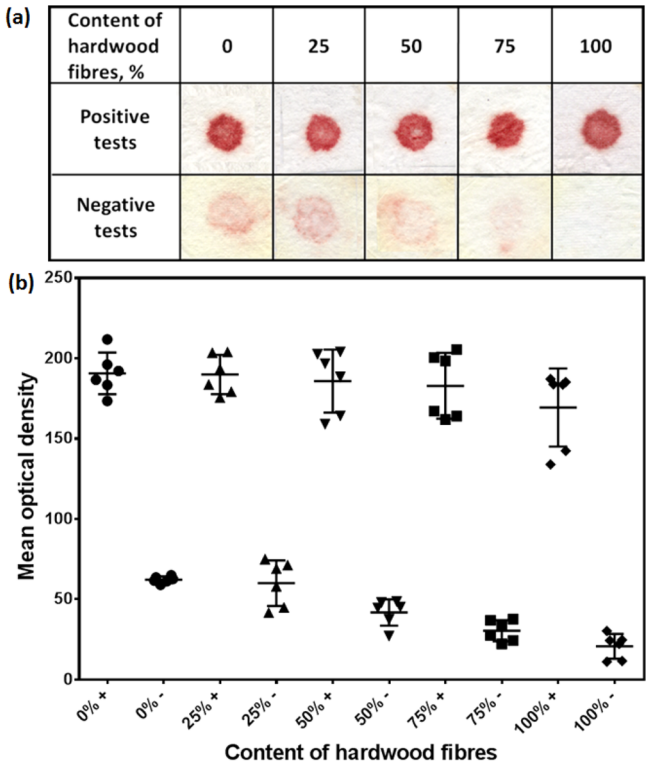

Figure 7. Vertical flow-through blood-typing tests using paper of different content of hardwood fibers: (a) scanned images of testing results and (b) mean optical densities of positive (+) or negative (−) tests.

Figure 6 and Table S5 (SI) support this analysis. For the rinsing method, the blood spot color densities of positive assays on sheets of different basis weights are different. This trend is different from that observed for the elution method. The slightly higher optical density of a positive result on 20 g/m^2 softwood than on 20 g/m^2 hardwood sheets can be attributed to the higher complexity of the internal pore structure in the softwood sheet compared with the hardwood sheet; complex pore structures make the movement of agglutinated RBCs in fiber network difficult.

For negative assays, hardwood fiber sheets show higher clarity than do softwood fiber sheets. This result can also be attributed to the structures of the fiber network. The less complex pore structures of hardwood fibers allow easy movement of RBCs with the rinsing buffer to travel through the sheets. Again, the more complex pore structure of the softwood fiber sheets makes RBC movement more difficult.

The blood-typing assay performances of all 20 g/m^2 mixed fiber sheets are shown in Figure 7. According to the above analysis, it can be understood that the color density of all positive assays is not significantly dependent on fiber mixing. However, the color density of negative assays is affected by the content of softwood fibers because of the increasing complexity in the sheet pore structure as the softwood fiber content increases.

In summary, the future design of paper sheets for buffer rinsing or flow-through blood-typing sensors will need to follow the principle using a low basis weight sheet with low content of softwood fibers.

4. CONCLUSIONS

In this study, we identified two important paper sheet physical properties that significantly influence the RBC transport behavior in paper: the fiber type and the sheet's internal pore structures. These properties must be controlled in paper sheet design for blood analysis applications. Low basis weight papers made with hardwood fibers have high porosities (i.e., the void fraction) and a simple internal pore structure. These properties, particularly the simple internal pore structure, allow the easy transport of RBCs in paper. Sensors made with such paper deliver high-clarity assay results. However, papers made with softwood fibers have lower porosity, and mercury porosimetry data revealed more complex sheet internal pore structures. Complex pore structures do not allow the easy transport of RBCs; thus, paper sheets made of softwood fibers have an inferior blood-typing performance compared with sheets made of hardwood fibers. Our analysis suggests that the number of fiber−fiber contacts along a single fiber in a sheet is likely to be a significant factor that affects the RBC transport. This analysis is made on the basis of the aqueous liquid flow pattern in paper that was previously reported. The liquid penetration front in a fiber network may be slowed down when it hits a discontinuity in its flow path, and fiber−fiber contacts in paper were identified by Roberts et al. as discontinuities for liquid penetration. Softwood fibers are much longer and thicker than hardwood fibers; the number of fiber−fiber contacts on a single softwood fiber is therefore greater than those on a single hardwood fiber in a paper sheet. RBC transport in softwood paper is therefore more difficult. The finding of this work will be used as a guide for future paper sheet design for paper-based blood analysis sensors.

For future work, more pulping and papermaking parameters including refining and addition of papermaking chemicals could be investigated.

■ ASSOCIATED CONTENT

Supporting Information

Basis weight, apparent thickness, and bulk of handsheets; statistical analysis of mean optical density of positive or negative lateral chromatographic elution blood-typing tests; and statistical analysis of mean optical density of positive or negative vertical washing blood typing tests (Tables S1–S6). This material is available free of charge via the Internet at http://pubs.acs.org.

■ AUTHOR INFORMATION

Corresponding Author

*Tel:+61-3-99053447. E-mail: wei.shen@monash.edu.

Notes

The authors declare no competing financial interest.

■ ACKNOWLEDGMENTS

This work is supported by Australian Research Council Grants (ARC DP1094179 and LP110200973). The authors thank Haemokinesis for its support through an ARC Linkage Project. L.L. thanks the Monash University Research and Graduate School and the Faculty of Engineering for postgraduate research scholarships.

■ REFERENCES

(1) Li, X.; Ballerini, D. R.; Shen, W. A Perspective on Paper-Based Microfluidics: Current Status and Future Trends. *Biomicrofluidics* **2012**, *6*, 11301–1130113.

(2) Abe, K.; Kotera, K.; Suzuki, K.; Citterio, D. Inkjet-Printed Paper Fluidic Immuno-Chemical Sensing Device. *Anal. Bioanal. Chem.* **2010**, *398*, 885–893.

(3) Delaney, J. L.; Hogan, C. F.; Tian, J.; Shen, W. Electrogenerated Chemiluminescence Detection in Paper-Based Microfluidic Sensors. *Anal. Chem.* **2011**, *83*, 1300–1306.

(4) Delaney, J. L.; Doeven, E. H.; Harsant, A. J.; Hogan, C. F. Use of a Mobile Phone for Potentiostatic Control with Low Cost Paper-Based Microfluidic Sensors. *Anal. Chim. Acta* **2013**, *790*, 56–60.

(5) Zhu, Y.; Xu, X.; Brault, N. D.; Keefe, A. J.; Han, X.; Deng, Y.; Xu, J.; Yu, Q.; Jiang, S. Cellulose Paper Sensors Modified with Zwitterionic Poly(carboxybetaine) for Sensing and Detection in Complex Media. *Anal. Chem.* **2014**, *86*, 2871–2875.

(6) Joo-Hyung, K.; Seongcheol, M.; Hyun, U. K.; Gyu-Young, Y.; Jaehwan, K. Disposable Chemical Sensors and Biosensors Made on Cellulose Paper. *Nanotechnology* **2014**, *25*, 092001.

(7) Kang, T.-K. Tunable Piezoresistive Sensors Based on Pencil-on-Paper. *Appl. Phys. Lett.* **2014**, *104*, 073117–073117–3.

(8) Khan, M. S.; Thouas, G.; Shen, W.; Whyte, G.; Garnier, G. Paper Diagnostic for Instantaneous Blood Typing. *Anal. Chem.* **2010**, *82*, 4158–4164.

(9) Nery, E. W.; Kubota, L. T. Sensing Approaches on Paper-Based Devices: A Review. *Anal. Bioanal. Chem.* **2013**, *405*, 7573–7595.

(10) Santhiago, M.; Nery, E. W.; Santos, G. P.; Kubota, L. T. Microfluidic Paper-Based Devices for Bioanalytical Applications. *Bioanalysis* **2014**, *6*, 89–106.

(11) Pelton, R. Bioactive Paper Provides a Low-Cost Platform for Diagnostics. *Trends Anal. Chem.* **2009**, *28*, 925–942.

(12) Biermann, C. J. *Handbook of Pulping and Papermaking*, 2nd ed.; Academic Press: New York, 1996.

(13) Ek, M.; Gellerstedt, G.; Henriksson, G. *Paper Chemistry and Technology*; Walter de Gruyter: Berlin, 2009.

(14) Li, X.; Tian, J.; Nguyen, T.; Shen, W. Paper-Based Microfluidic Devices by Plasma Treatment. *Anal. Chem.* **2008**, *80*, 9131–9134.

(15) Li, X.; Tian, J.; Garnier, G.; Shen, W. Fabrication of Paper-Based Microfluidic Sensors by Printing. *Colloids Surf., B* **2010**, *76*, 564–570.

(16) Martinez, A. W.; Phillips, S. T.; Butte, M. J.; Whitesides, G. M. Patterned Paper as a Platform for Inexpensive, Low-Volume, Portable Bioassays. *Angew. Chem.* **2007**, *119*, 1340–1342.

(17) Ballerini, D.; Li, X.; Shen, W. Patterned Paper and Alternative Materials as Substrates for Low-Cost Microfluidic Diagnostics. *Microfluid Nanofluid* **2012**, *13*, 769–787.

(18) Al-Tamimi, M.; Shen, W.; Zeineddine, R.; Tran, H.; Garnier, G. Validation of Paper-Based Assay for Rapid Blood Typing. *Anal. Chem.* **2012**, *84*, 1661–8.

(19) Li, M. S.; Tian, J. F.; Al-Tamimi, M.; Shen, W. Paper-Based Blood Typing Device That Reports Patient's Blood Type "in Writing". *Angew. Chem. Int. Ed.* **2012**, *51*, 5497–5501.

(20) Li, H.; Han, D.; Pauletti, G. M.; Steckl, A. J. Blood Coagulation Screening Using a Paper-Based Microfluidic Lateral Flow Device. *Lab Chip* **2014**, *14*, 4035–4041.

(21) Lee, C. H.; Tian, L.; Singamaneni, S. Paper-Based SERS Swab for Rapid Trace Detection on Real-World Surfaces. *ACS Appl. Mater. Interfaces* **2010**, *2*, 3429–3435.

(22) Noor, M. O.; Krull, U. J. Paper-Based Solid-Phase Multiplexed Nucleic Acid Hybridization Assay with Tunable Dynamic Range Using Immobilized Quantum Dots as Donors in Fluorescence Resonance Energy Transfer. *Anal. Chem.* **2013**, *85*, 7502–7511.

(23) Ek, M.; Gellerstedt, G.; Henriksson, G. *Paper Products Physics and Technology*; Walter de Gruyter: Berlin, 2009.

(24) Niskanen, K. J. *Paper Physics*; Fapet Oy: Helsinki, Finland, 1999.

(25) Jarujamrus, P.; Tian, J. F.; Li, X.; Siripinyanond, A.; Shiowatana, J.; Shen, W. Mechanisms of Red Blood Cells Agglutination in Antibody-Treated Paper. *Analyst* **2012**, *137*, 2205–2210.

(26) Daniels, G.; Reid, M. E. Blood Groups: The Past 50 Years. *Transfusion* **2010**, *50*, 281–289.

(27) Duguid, J. K. M.; Bromilow, I. M. New Technology in Hospital Blood Banking. *J. Clin. Pathol.* **1993**, *46*, 585–588.

(28) Daniels, G.; Bromilow, I. M. *Essential Guide to Blood Groups*; Wiley-Blackwell: Chichester, UK, 2010.

(29) Li, L.; Tian, J.; Ballerini, D.; Li, M.; Shen, W. A Study of the Transport and Immobilisation Mechanisms of Human Red Blood Cells in a Paper-Based Blood Typing Device Using Confocal Microscopy. *Analyst* **2013**, *138*, 4933–4940.

(30) Paulapuro, H. *Papermaking Part 1, Stock Preparation and Wet End*, 2nd ed.; Fapet: Helsinki, Finland, 2008; Vol. *8*.

(31) Alén, R. *Papermaking Chemistry*; Fapet: Helsinki, Finland, 2007; Vol. *4*.

(32) Levlin, J.; Soderhjelm, L. *Pulp and Paper Testing*; Fapet: Helsinki, Finland, 1999; Vol. *17*.

(33) Silvy, J.; Pannier, C.; Veyre, J. *16th EUCEPA Conference Proceedings*; Paper Industry Technical Association: Bury, UK,1976.

(34) Webb, P. A.; Orr, C. *Analytical Methods in Fine Particle Technology*; Micromeritics Instrument Corp.: Norcross, GA,1997.

(35) Reinhart, W. H.; Chien, S. Roles of Cell Geometry and Cellular-Viscosity in Red-Cell Passage through Narrow Pores. *Am. J. Physiol.* **1985**, *248*, C473–C479.

(36) Gong, X.; Sugiyama, K.; Takagi, S.; Matsumoto, Y. The Deformation Behavior of Multiple Red Blood Cells in a Capillary Vessel. *J. Biomech. Eng.* **2009**, *131*, 074504–074504.

(37) Roberts, R. J.; Senden, T. J.; Knackstedt, M. A.; Lyne, M. B. Spreading of Aqueous Liquids in Unsized Papers is by Film Flow. *J. Pulp Pap. Sci.* **2003**, *29*, 123–131.

(38) Fardim, P. *Chemical Pulping*; Fapet: Helsinki, Finland, 1999; Vol. *6*.

(39) He, J.; Batchelor, W.; Johnston, R. An Analytical Model for Number of Fibre–Fibre Contacts in Paper and Expressions for Relative Bonded Area (RBA). *J. Mater. Sci.* **2007**, *42*, 522–528.

(40) Batchelor, W. J.; He, J.; Sampson, W. W. Inter-Fibre Contacts in Random Fibrous Materials: Experimental Verification of Theoretical Dependence on Porosity and Fibre Width. *J. Mater. Sci.* **2006**, *41*, 8377–8381.